Energy levels, radiative rates, and electron impact excitation rates for transitions in OVII

A&A 489, 1377–1388 (2008)
DOI: 10.1051/0004-6361:200810531

Astronomy & Astrophysics

Energy levels, radiative rates, and electron impact excitation rates for transitions in O VII⋆

K. M. Aggarwal and F. P. Keenan

Astrophysics Research Centre, School of Mathematics and Physics, Queen's University Belfast, Belfast BT7 1NN, Northern Ireland, UK
e-mail: K.Aggarwal@qub.ac.uk

Received 7 July 2008 / Accepted 7 August 2008

ABSTRACT

Aims. In this paper we report calculations for energy levels, radiative rates, and electron impact excitation rates for transitions in O VII.
Methods. The GRASP (general-purpose relativistic atomic structure package) is adopted for calculating energy levels and radiative rates. For determining the collision strengths and subsequently the excitation rates, the Dirac atomic R-matrix code (DARC) and the flexible atomic code (FAC) are used.
Results. Oscillator strengths, radiative rates, and line strengths are reported for all E1, E2, M1, and M2 transitions among the lowest 49 levels of O VII. Collision strengths have been averaged over a Maxwellian velocity distribution, and the resulting effective collision strengths are reported over a wide temperature range below 2×10^6 K. Additionally, lifetimes are also listed for all levels.

Key words. atomic data – atomic processes

1. Introduction

Emission lines of He-like O VII have been widely observed in a variety of astrophysical and laboratory plasmas. For example, lines in the X-ray region (1–50 Å) have been detected in solar flares by McKenzie et al. (1980) and Phillips et al. (1999), as listed by Dere et al. (2001). Similarly, Winkler et al. (1981) have observed some lines in the X-ray region from supernova remnants. Of particular interest are the resonance (w:1s^2 ^{1}S$_0$–1s2p ^{1}P$^\circ_1$), intercombination (x and y: 1s^2 ^{1}S$_0$–1s2p ^{3}P$^\circ_{2,1}$), and forbidden (z: 1s^2 ^{1}S$_0$–1s2s ^{3}S$_1$) lines, which are highly useful for solar plasma diagnostics – see, for example, Gabriel & Jordan (1969) and Acton et al. (1972). Keenan et al. (1985) have also shown that the 1s^2 ^{1}S–2snp ^{1}P (n = 2–4) emission lines of O VII provide electron temperature estimates for the solar corona. Similarly, emission lines of O VII have been detected in the 15–140 Å region by Isler et al. (1993), using spectra recorded at the ISX-A tokamak at Oak Ridge National Laboratory (ORNL), and by Baker (1993) in a theta-pinch plasma in the 1600–2500 Å wavelength range. However, to reliably analyse observations, atomic data are required for many parameters, such as: energy levels, radiative rates (A-values), and excitation rates or equivalently the effective collision strengths (Υ), which are obtained from the electron impact collision strengths (Ω). Since experimental values are not available for the desired atomic parameters, except for energy levels, theoretical results are required.

Due to the wide variety of O VII observations and the diagnostic potential of lines from this ion, several calculations of atomic data are available in the literature. However, the most recent and comprehensive are by Delahaye & Pradhan (2002), who adopted the SuperStructure (SS) program of Eissner et al. (1974) for the generation of wavefunctions, and the Breit-Pauli R-matrix program of Berrington et al. (1995) for the computation of collision strengths (Ω) and subsequently effective collision strengths (Υ). They calculated values of Ω over a wide energy range below 200 Ryd, resolved resonances in the threshold region, and determined values of Υ over a wide temperature range of 10^4–10^7 K. Furthermore, they included one-body relativistic operators in the generation of wavefunctions as well as in the scattering process. Therefore, their results should be the most accurate available today. However, their calculations are confined to the $n \leq 4$ levels alone, whereas transitions involving the $n = 5$ levels have been observed (Dere et al. 2001). Furthermore, Delahaye & Pradhan presented only representative results for a few transitions, although their results for Υ are available electronically on the TIPbase (http://vizier.u-strasbg.fr/tipbase/home.html). Therefore, our aim is to extend the calculations of Delahaye & Pradhan by also including the $n = 5$ levels, and to report a complete set of results (namely energy levels, radiative rates, and effective collision strengths) for all transitions among the lowest 49 levels of O VII. Finally, we also report the A-values for four types of transitions, namely electric dipole (E1), electric quadrupole (E2), magnetic dipole (M1), and magnetic quadrupole (M2), because these are also required for plasma modelling.

Furthermore, our approach is fully relativistic, as for the determination of wavefunctions we have employed the *general-purpose relativistic atomic structure package* (GRASP), originally developed by Grant et al. (1980) and revised by Dr. Norrington. It is a fully relativistic code, based on the jj coupling scheme. Further relativistic corrections arising from the Breit interaction and QED effects have also been included. Additionally, we have used the option of *extended average level* (EAL), in which a weighted (proportional to $2j+1$) trace of the Hamiltonian matrix is minimized. This produces a compromise

⋆ Tables 2 and 6 are only available in electronic form at the CDS via anonymous ftp to cdsarc.u-strasbg.fr (130.79.128.5) or via http://cdsweb.u-strasbg.fr/cgi-bin/qcat?J/A+A/489/1377

Table 1. Energy levels (in Ryd) of O VII.

Index	Configuration/Level		NIST	GRASP1	GRASP2	FAC1	FAC2	SS	MBPT
1	$1s^2$	$^1S_0$	0.00000	0.00000	0.00000	0.00000	0.00000	0.0000	0.00000
2	1s2s	$^3S_1$	41.23155	41.05246	41.03508	41.14868	41.14842	41.2438	41.23949
3	1s2p	$^3P^o_0$	41.78724	41.61135	41.59725	41.73910	41.73896	41.7933	41.79607
4	1s2p	$^3P^o_1$	41.78779	41.61434	41.59775	41.73960	41.73946	41.7942	41.79660
5	1s2p	$^3P^o_2$	41.79280	41.62044	41.60273	41.74439	41.74425	41.7997	41.80161
6	1s2s	$^1S_0$	41.81240	41.66296	41.64791	41.77554	41.77529	41.8074	41.81546
7	1s2p	$^1P^o_1$	42.18438	42.01968	42.00142	42.17212	42.17198	42.2100	42.18790
8	1s3s	$^3S_1$	48.65091	48.46935	48.45154	48.58117	48.58100	48.6577	48.66068
9	1s3p	$^3P^o_0$	48.80446	48.62106	48.60415	48.73673	48.73664	48.8114	48.81207
10	1s3p	$^3P^o_1$	48.80446	48.62193	48.60435	48.73697	48.73688	48.8116	48.81227
11	1s3p	$^3P^o_2$	48.80446	48.62371	48.60583	48.73844	48.73835	48.8132	48.81376
12	1s3s	$^1S_0$	48.81129	48.63498	48.61790	48.74376	48.74357	48.8217	48.81306
13	1s3d	$^3D_1$	48.88374	48.70037	48.68262	48.80681	48.80681	48.8930	48.89282
14	1s3d	$^3D_2$	48.88428	48.70065	48.68270	48.80689	48.80689	48.8931	48.89289
15	1s3d	$^3D_3$	48.88437	48.70116	48.68315	48.80732	48.80732	48.8935	48.89335
16	1s3d	$^1D_2$	48.89376	48.70506	48.68714	48.81229	48.81229	48.8971	48.89682
17	1s3p	$^1P^o_1$	48.92183	48.73674	48.71873	48.85493	48.85482	48.9281	48.92119
18	1s4s	$^3S_1$	51.17986	50.98944	50.97156	51.09360	51.09344	51.1813	51.18171
19	1s4p	$^3P^o_0$	51.23690	51.05146	51.03394	51.14996	51.14988	51.2436	51.24367
20	1s4p	$^3P^o_1$	51.23690	51.05183	51.03404	51.15008	51.15000	51.2437	51.24377
21	1s4p	$^3P^o_2$	51.23690	51.05258	51.03466	51.15072	51.15063	51.2444	51.24440
22	1s4s	$^1S_0$	51.24146	51.05811	51.04055	51.15922	51.15902	51.2475	51.24341
23	1s4d	$^3D_1$	51.26752	51.08411	51.06626	51.19366	51.19366	51.2767	51.27697
24	1s4d	$^3D_2$	51.26788	51.08424	51.06630	51.19370	51.19370	51.2767	51.27700
25	1s4d	$^3D_3$	51.27244	51.08445	51.06648	51.19385	51.19385	51.2769	51.27719
26	1s4f	$^3F^o_2$		51.08597	51.06807	51.18727	51.18727	51.2786	51.27905
27	1s4f	$^3F^o_3$		51.08598	51.06802	51.18723	51.18723	51.2785	51.27900
28	1s4f	$^3F^o_4$	51.26980	51.08614	51.06818	51.18739	51.18739	51.2787	
29	1s4f	$^1F^o_3$	51.27554	51.08615	51.06824	51.18746	51.18746	51.2787	51.27922
30	1s4d	$^1D_2$	51.27399	51.08662	51.06869	51.19656	51.19656	51.2790	51.27909
31	1s4p	$^1P^o_1$	51.28702	51.09990	51.08194	51.19849	51.19838	51.2916	51.28866
32	1s5s	$^3S_1$	52.33051	52.13981	52.12190	52.24041	52.24020		52.33229
33	1s5p	$^3P^o_0$	52.35630	52.17106	52.15333	52.26805	52.26793		52.36350
34	1s5p	$^3P^o_1$	52.35630	52.17125	52.15339	52.26811	52.26799		52.36359
35	1s5p	$^3P^o_2$	52.35630	52.17163	52.15371	52.26844	52.26831		52.36398
36	1s5s	$^1S_0$		52.17550	52.15778	52.27342	52.27311		52.36325
37	1s5d	$^3D_1$	52.37416	52.18755	52.16965	52.29583	52.29583		52.38054
38	1s5d	$^3D_2$	52.37435	52.18761	52.16968	52.29585	52.29585		52.38056
39	1s5d	$^3D_3$	52.37617	52.18772	52.16977	52.29593	52.29593		52.38065
40	1s5f	$^3F^o_2$		52.18858	52.17066	52.28959	52.28959		52.38168
41	1s5f	$^3F^o_3$		52.18858	52.17064	52.28958	52.28958		52.38166
42	1s5f	$^3F^o_4$	52.37234	52.18866	52.17072	52.28965	52.28965		
43	1s5f	$^1F^o_3$	52.37799	52.18867	52.17075	52.28969	52.28969		52.38177
44	1s5g	$^3G_3$		52.18867	52.17075	52.28956	52.28956		52.38182
45	1s5g	$^3G_4$		52.18867	52.17073	52.28955	52.28955		
46	1s5g	$^3G_5$		52.18872	52.17078	52.28960	52.28960		
47	1s5g	$^1G_4$		52.18872	52.17080	52.28962	52.28962		
48	1s5d	$^1D_2$	52.38173	52.18895	52.17102	52.29745	52.29745		52.38173
49	1s5p	$^1P^o_1$	52.38373	52.19614	52.17819	52.29262	52.29246		52.38634

NIST: http://physics.nist.gov/PhysRefData. GRASP1: energies from the GRASP code with 49 level calculations *without* Breit and QED effects. GRASP2: energies from the GRASP code with 49 level calculations *with* Breit and QED effects. FAC1: energies from the FAC code with 49 level calculations. FAC2: energies from the FAC code with 71 level calculations. SS: energies of Delahaye & Pradhan (2002) from the SS code. MBPT: energies of Savukov et al. (2003) from the MBPT code.

set of orbitals describing closely lying states with moderate accuracy. Similarly, for our calculations of Ω, we have adopted the *Dirac atomic R-matrix code* (DARC) of Norrington & Grant (private communication). Finally, in order to assess the accuracy of our results, we have performed parallel calculations from the *Flexible Atomic Code* (FAC) of Gu (2003), available from the website http://kipac-tree.stanford.edu/fac. This is also a fully relativistic code which provides a variety of atomic parameters, and yields results comparable to GRASP and DARC. Thus, results from FAC will be helpful in assessing the accuracy of our energy levels, radiative rates, and collision strengths.

2. Energy levels

The $1s^2$, $1s2\ell$, $1s3\ell$, $1s4\ell$, and $1s5\ell$ configurations of O VII give rise to the lowest 49 levels listed in Table 1, where we compare our level energies from GRASP, obtained *without* and *with* the inclusion of Breit and QED effects, with the experimental

values compiled by NIST (National Institute of Standards and Technology), and available at their website http://physics.nist.gov/PhysRefData. Our level energies obtained without Breit and QED effects (GRASP1) are consistently lower than the experimental values by ∼0.2 Ryd, but are in agreement within 0.5%. However, the orderings are slightly different from those of NIST in a few instances, such as for levels 16, 30, and 42. The inclusion of Breit and QED effects (slightly) lowers the level energies by ∼0.02 Ryd (GRASP2), and hence comparatively increases the difference with the experimental values, but the agreement remains within 0.5%. Furthermore, the orderings have slightly altered in three instances, namely for levels 26/27, 40/41, and 43/45. However, the energy differences for these "swapping" levels are very small. Our level energies obtained from the FAC code (FAC1), including the same CI (configuration interaction) as in GRASP1, are consistently higher by ∼0.1 Ryd and hence are comparatively in better agreement with the NIST listings. The level orderings from FAC1 are also in agreement with our calculations from GRASP, except for the 1s5d ^{1}D$_2$ and 1s5p ^{1}P$^\circ_1$ levels (48 and 49). For these, our orderings from GRASP are in agreement with the experimental values. Other minor differences in level orderings from FAC1 are for the levels of the 1s5f and 1s5g configurations. A further inclusion of 1s6ℓ configurations, as in the FAC2 calculations, makes no difference either in magnitude or orderings, mainly because levels of the 1s6ℓ configurations lie *above* the lowest 49 levels listed in Table 1, and hence do not interact with these.

Other energy levels listed in Table 1 are from the SS calculations of Delahaye & Pradhan (2002) and those of Savukov et al. (2003) from relativistic many-body perturbation theory (MBPT). The energy levels of Delahaye & Pradhan are in better agreement with the experimental values, but are available only for the lowest 31 levels. Additionally, if we have a closer look at the energies of 1s2p ^{3}P$^\circ_{0,1,2}$, the level splittings of Delahaye & Pradhan differ considerably with the experimental and other theoretical results. Similarly, the energy levels of Savukov et al. are available for all the $J \leq 3$ levels, and are in better agreement with the experimental results, but only in magnitude. Their level orderings are different with our calculations and the NIST listings in many instances, such as for levels: 12, 22, 30, and particularly for level 48 (1s5d ^{1}D$_2$). Since most of the energy levels within any n complex are very close to one another, different calculations provide slightly different orderings. To conclude, we may state that overall there is no discrepancy between theory and experiment for the energy levels of O VII. However, experimental energies are not available for all the levels listed in Table 1, and the 1s3p ^{3}P$^\circ_{0,1,2}$, 1s4p ^{3}P$^\circ_{0,1,2}$, and 1s5p ^{3}P$^\circ_{0,1,2}$ levels are non-degenerate in energy. For such non-degenerate and missing levels, we recommend that our energy levels either from the GRASP2 or FAC1 calculations should be adopted in any plasma modelling applications. For the remaining levels, the experimentally compiled listings of the NIST should be preferred.

3. Radiative rates

The absorption oscillator strength (f_{ij}) and radiative rate A_{ji} (in s^{-1}) for a transition $i \rightarrow j$ are related by the following expression:

$$f_{ij} = \frac{mc}{8\pi^2 e^2}\lambda_{ji}^2 \frac{\omega_j}{\omega_i} A_{ji} = 1.49 \times 10^{-16} \lambda_{ji}^2 (\omega_j/\omega_i) A_{ji} \quad (1)$$

where m and e are the electron mass and charge, respectively, c is the velocity of light, λ_{ji} is the transition energy/wavelength in Å, and ω_i and ω_j are the statistical weights of the lower (i) and upper (j) levels, respectively. Similarly, the oscillator strength f_{ij} (dimensionless) and the line strength S (in atomic unit) are related by the standard equations listed below.

For the electric dipole (E1) transitions

$$A_{ji} = \frac{2.0261 \times 10^{18}}{\omega_j \lambda_{ji}^3} S^{\rm E1} \quad \text{and} \quad f_{ij} = \frac{303.75}{\lambda_{ji}\omega_i} S^{\rm E1}, \quad (2)$$

for the magnetic dipole (M1) transitions

$$A_{ji} = \frac{2.6974 \times 10^{13}}{\omega_j \lambda_{ji}^3} S^{\rm M1} \quad \text{and} \quad f_{ij} = \frac{4.044 \times 10^{-3}}{\lambda_{ji}\omega_i} S^{\rm M1}, \quad (3)$$

for the electric quadrupole (E2) transitions

$$A_{ji} = \frac{1.1199 \times 10^{18}}{\omega_j \lambda_{ji}^5} S^{\rm E2} \quad \text{and} \quad f_{ij} = \frac{167.89}{\lambda_{ji}^3\omega_i} S^{\rm E2}, \quad (4)$$

and for the magnetic quadrupole (M2) transitions

$$A_{ji} = \frac{1.4910 \times 10^{13}}{\omega_j \lambda_{ji}^5} S^{\rm M2} \quad \text{and} \quad f_{ij} = \frac{2.236 \times 10^{-3}}{\lambda_{ji}^3\omega_i} S^{\rm M2}. \quad (5)$$

In Table 2 we present transition energies/wavelengths (λ, in Å), radiative rates (A_{ji}, in s^{-1}) , oscillator strengths (f_{ij}, dimensionless), and line strengths (S, in au), in length form only, for all 336 electric dipole (E1) transitions among the 49 levels of O VII. The *indices* used to represent the lower and upper levels of a transition have already been defined in Table 1. Similarly, there are 391 electric quadrupole (E2), 316 magnetic dipole (M1), and 410 magnetic quadrupole (M2) transitions among the 49 levels. However, for these transitions only the A-values are listed in Table 2, and the corresponding results for f- or S-values can be easily obtained using Eqs. (1)–(5).

In Table 3 we compare our radiative rates (A-values), both from GRASP and FAC, with those of Delahaye & Pradhan (2002) from the SS code, Savukov et al. (2003) from MBPT, and of those listed on the NIST website, for the common E1 transitions. Generally, all sets of A-values agree within 10%, although for some weak transitions, such as: 2–5, 6–7, and 12–17, differences are up to 20%, and for the 16–17 (1s3d ^{1}D$_2$–1s3p ^{1}P$^\circ_1$, $f = 0.0085$) transition, the discrepancy is up to a factor of two. For this transition our A-value is the highest whereas those of Savukov et al. is the lowest. This is because weak transitions are very sensitive to mixing coefficients, and hence differing amount of CI (and methods) produce different A-values, as discussed in detail by Hibbert (2000). However, we would like to emphasize here that although A-values for weak transitions are also required in modelling applications, their contribution is usually not very important in comparison to stronger transitions with $f \geq 0.01$.

One of the general criteria to assess the accuracy of radiative rates is to compare the length and velocity forms of the f- or A-values. However, such comparisons are only desirable, and are *not* a fully sufficient test to assess accuracy, as different calculations (or combinations of configurations) may give comparable f-values in the two forms, but entirely different results in magnitude. Generally, there is a good agreement between the length and velocity forms of the f-values for *strong* transitions, but differences between the two forms can sometimes be substantial even for some very strong transitions, as demonstrated through

Table 3. Comparison of A-values (in s^{-1}) for some transitions of O VII. $a \pm b \equiv a \times 10^{\pm b}$.

i	j	NIST	GRASP	FAC	SS	MBPT
1	7	3.309 + 12	3.4949 + 12	3.408 + 12	3.403 + 12	3.302 + 12
1	17	9.365 + 11	1.1027 + 12	9.958 + 11	1.004 + 12	9.345 + 11
2	3	7.797 + 07	8.3043 + 07	9.537 + 07	8.058 + 07	7.940 + 07
2	4	7.820 + 07	8.3276 + 07	9.562 + 07	8.083 + 07	7.964 + 07
2	5	8.033 + 07	8.5585 + 07	9.807 + 07	8.309 + 07	8.188 + 07
3	8	2.505 + 09	2.4036 + 09	2.311 + 09	2.237 + 09	2.519 + 09
3	13	8.982 + 10	8.9564 + 10	8.814 + 10	8.927 + 10	8.969 + 10
4	8	7.512 + 09	7.1885 + 09	6.912 + 09	6.739 + 09	7.538 + 09
4	13	6.735 + 10	6.7164 + 10	6.610 + 10	6.699 + 10	6.726 + 10
4	14	1.213 + 11	1.1973 + 11	1.183 + 11	1.205 + 11	1.196 + 11
5	8	1.249 + 10	1.2021 + 10	1.156 + 10	1.131 + 10	1.261 + 10
5	13	4.481 + 09	4.4734 + 09	4.402 + 09	4.466 + 09	4.480 + 09
5	14	4.033 + 10	3.9761 + 10	3.930 + 10	4.012 + 10	3.969 + 10
5	15	1.613 + 11	1.6109 + 11	1.586 + 11	1.608 + 11	1.613 + 11
6	7	2.514 + 07	2.1567 + 07		2.509 + 07	2.548 + 07
6	17	5.055 + 10	5.2792 + 10	5.121 + 10	5.209 + 10	5.039 + 10
7	12	2.008 + 10	2.2082 + 10	2.077 + 10	2.223 + 10	2.014 + 10
7	16	1.523 + 11	1.5139 + 11	1.487 + 11	1.540 + 11	1.503 + 11
9	13	6.114 + 05	5.9952 + 05		6.200 + 05	6.523 + 05
10	13	4.585 + 05	4.4635 + 05		4.649 + 05	4.857 + 05
10	14	8.426 + 05	7.9793 + 05		8.535 + 05	8.656 + 05
11	13	3.057 + 04	2.8024 + 04		3.099 + 04	3.054 + 04
11	14	2.809 + 05	2.5043 + 05		2.841 + 05	2.719 + 05
11	15	1.127 + 06	1.0327 + 06		1.143 + 06	1.125 + 06
12	17	3.864 + 06	3.0023 + 06		3.958 + 06	3.739 + 06
16	17	7.410 + 04	1.1423 + 05		8.082 + 04	5.238 + 08

NIST: http://physics.nist.gov/PhysRefData. GRASP: present 49 level calculations from the GRASP code. FAC: present 49 level calculations from the FAC code. SS: calculations of Delahaye & Pradhan (2002) from the SS code. MBPT: calculations of Savukov et al. (2003) from the MBPT code.

various examples by Aggarwal et al. (2007). Nevertheless, for almost all of the strong transitions ($f \geq 0.01$) the two forms agree to within 20%, but differences for 11 (<4%) transitions are higher by up to a factor of two. Additionally, for two transitions (6–7: $f = 0.064$ and 48–49: $f = 0.023$), the two forms differ by factors of 3 and 6, respectively. However, for both of these transition energies (ΔE) are very small, and a slight variation in ΔE affects the A-values considerably. Therefore, on the basis of these comparisons and discussion we may state that for a majority of the strong E1 transitions, our radiative rates are accurate to better than 20%. However, for the weaker transitions this assessment of accuracy does not apply.

4. Lifetimes

The lifetime τ for a level j is defined as follows:

$$\tau_j = \frac{1}{\sum_i A_{ji}} \cdot \tag{6}$$

Since this is a measurable parameter, it provides a check on the accuracy of the calculations. Therefore, in Table 4 we have listed our calculated lifetimes, which *include* the contributions from four types of transitions, i.e. E1, E2, M1, and M2. Also included in this table are the theoretical results of Savukov et al. (2003) from MBPT and some early measurements by Träbert et al. (1977) from beam-foil spectra.

In general, agreement between our present and earlier (Savukov et al. 2003) theoretical lifetimes is better than 20% for most of the levels, but the differences are larger for a few levels, such as 6, 36, and 49. Since for level 6 ($1s2s\ ^1S_0$) both the magnitude of the lifetime as well as the discrepancy is the highest (over an order of magnitude), we focus on this level alone. The maximum contribution for this level comes from the 4-6 E1 transition, for which our A-value is 25.69 s^{-1}, whereas that of Savukov et al. is 1.435 s^{-1}. However, the 4–6 transition is very weak ($f = 4.24 \times 10^{-7}$), and hence accuracy estimates are always insecure (Hibbert 2000). Nevertheless, our above f-value from GRASP compares reasonably well (within a factor of two) with the corresponding FAC calculations, but the corresponding difference in the A-values is a factor of three. This is because the A- and f-values have a ΔE^2 (or equivalently λ_{ji}^2) dependence as seen already in Eq. (1), and therefore any difference in ΔE has a larger effect on the A- value. The experimental value of ΔE for the 4–6 transition is 0.02461 Ryd, and the corresponding values from GRASP, FAC, and MBPT are 0.0502, 0.03594, and 0.01886 Ryd, respectively. Therefore, an approximate "correction" to the A-values can be applied (Hibbert 1996) by multiplying these by the $(\Delta E_{\rm exp}/\Delta E_{\rm the})^2$ factor. Following this, the A-values from GRASP, FAC, and MBPT are 6.174 s^{-1}, 3.671 s^{-1}, and 2.443 s^{-1}, or the τ values are 0.162 s, 0.272 s, and 0.409 s, respectively. As a result, the discrepancy for the τ values among three independent calculations is now within a factor of 2.5. A measurement of a lifetime for the $1s2s\ ^1S_0$ level will be helpful to resolve the discrepancy.

For the levels for which experimental values of τ are available, the agreement is within the limits of uncertainty, except for level 8 ($1s3s\ ^3S_1$) for which the discrepancy is ~40%. Overall we may state that there is good agreement between the theoretical and experimental lifetimes for a majority of the levels.

5. Collision strengths

For the computation of collision strengths Ω, we have employed the *Dirac atomic R-matrix code* (DARC), which includes the

Table 4. Comparison of theoretical and experimental lifetimes (τ in s) for the levels of O VII. $a{-}b \equiv a \times 10^{-b}$.

Level	Configuration/Level		GRASP	MBPT	Experimental
2	1s2s	$^3S_1$	1.061−03	9.535−04	
3	1s2p	$^3P^\circ_0$	1.204−08	1.259−08	
4	1s2p	$^3P^\circ_1$	1.598−09	1.625−09	
5	1s2p	$^3P^\circ_2$	1.164−08	1.216−08	
6	1s2s	$^1S_0$	3.890−02	6.885−01	
7	1s2p	$^1P^\circ_1$	2.861−13	3.029−13	
8	1s3s	$^3S_1$	4.627−11	4.412−11	(6.5 ± 0.6) −11
9	1s3p	$^3P^\circ_0$	1.924−11	1.879−11	(1.92 ± 0.2)−11
10	1s3p	$^3P^\circ_1$	1.918−11	1.874−11	(1.92 ± 0.2)−11
11	1s3p	$^3P^\circ_2$	1.928−11	1.883−11	(1.92 ± 0.2)−11
12	1s3s	$^1S_0$	4.528−11	4.965−11	
13	1s3d	$^3D_1$	6.203−12	6.194−12	(7.0 ± 2.0) −12
14	1s3d	$^3D_2$	6.207−12	6.199−12	(7.0 ± 2.0) −12
15	1s3d	$^3D_3$	6.207−12	6.198−12	(7.0 ± 2.0) −12
16	1s3d	$^1D_2$	6.528−12	6.555−12	(8.0 ± 1.5) −12
17	1s3p	$^1P^\circ_1$	8.654−13	1.015−12	
18	1s4s	$^3S_1$	7.303−11	6.611−11	
19	1s4p	$^3P^\circ_0$	3.322−11	3.163−11	(3.12 ± 0.2)−11
20	1s4p	$^3P^\circ_1$	3.313−11	3.156−11	(3.12 ± 0.2)−11
21	1s4p	$^3P^\circ_2$	3.329−11	3.168−11	(3.12 ± 0.2)−11
22	1s4s	$^1S_0$	5.692−11	7.286−11	
23	1s4d	$^3D_1$	1.441−11	1.431−11	(1.6 ± 0.15)−11
24	1s4d	$^3D_2$	1.442−11	1.432−11	(1.6 ± 0.15)−11
25	1s4d	$^3D_3$	1.442−11	1.432−11	(1.6 ± 0.15)−11
26	1s4f	$^3F^\circ_2$	3.015−11	3.014−11	
27	1s4f	$^3F^\circ_3$	3.016−11	3.016−11	
28	1s4f	$^3F^\circ_4$	3.015−11		
29	1s4f	$^1F^\circ_3$	3.018−11	3.018−11	
30	1s4d	$^1D_2$	1.507−11	1.543−11	(1.62 ± 0.15)−11
31	1s4p	$^1P^\circ_1$	1.712−12	2.395−12	
32	1s5s	$^3S_1$	1.336−10	1.056−10	
33	1s5p	$^3P^\circ_0$	6.074−11	5.358−11	
34	1s5p	$^3P^\circ_1$	6.053−11	5.349−11	
35	1s5p	$^3P^\circ_2$	6.090−11	5.366−11	
36	1s5s	$^1S_0$	6.079−11	1.151−10	
37	1s5d	$^3D_1$	2.832−11	2.744−11	(3.1 ± 0.3) −11
38	1s5d	$^3D_2$	2.833−11	2.746−11	(3.1 ± 0.3) −11
39	1s5d	$^3D_3$	2.837−11	2.754−11	(3.1 ± 0.3) −11
40	1s5f	$^3F^\circ_2$	5.829−11	5.828−11	
41	1s5f	$^3F^\circ_3$	5.832−11	5.833−11	
42	1s5f	$^3F^\circ_4$	5.831−11		
43	1s5f	$^1F^\circ_3$	5.836−11	5.838−11	
44	1s5g	$^3G_3$	9.782−11	9.795−11	
45	1s5g	$^3G_4$	9.782−11		
46	1s5g	$^3G_5$	9.783−11		
47	1s5g	$^1G_4$	9.784−11		
48	1s5d	$^1D_2$	2.664−11	2.982−11	(2.8 ± 0.2) −11
49	1s5p	$^1P^\circ_1$	2.316−12	4.660−12	

GRASP: Present 49 level calculations from the GRASP code. MBPT: calculations of Savukov et al. (2003) from the MBPT code. Expt: measurements for the *LS* states by Trabert et al. (1977).

relativistic effects in a systematic way, in both the target description and the scattering model. It is based on the *jj* coupling scheme, and uses the Dirac-Coulomb Hamiltonian in the *R*-matrix approach. The *R*-matrix radius has been adopted to be 14.24 au, and 55 continuum orbitals have been included for each channel angular momentum for the expansion of the wavefunction. This allows us to compute Ω up to an energy of 80 Ryd, sufficient to calculate the excitation rates up to a temperature of 10^6 K. The maximum number of channels for a partial wave is 217, and the corresponding size of the Hamiltonian matrix is 11991. In order to obtain convergence of Ω for all transitions and at all energies, we have included all partial waves with angular momentum $J \leq 40.5$, although a larger number would have been preferable for the convergence of some allowed transitions, especially at higher energies. However, to account for the inclusion of higher neglected partial waves, we have included a top-up, based on the Coulomb-Bethe approximation for allowed transitions and geometric series for others.

In Figs. 1–3 we show the variation of Ω with angular momentum J for three transitions, namely 2–4 (1s2s $^3S_1$–1s2p $^3P^\circ_1$), 2–10 (1s2s $^3S_1$–1s3p $^3P^\circ_1$), and 9–11 (1s3p $^3P^\circ_0$–1s3p $^3P^\circ_2$),

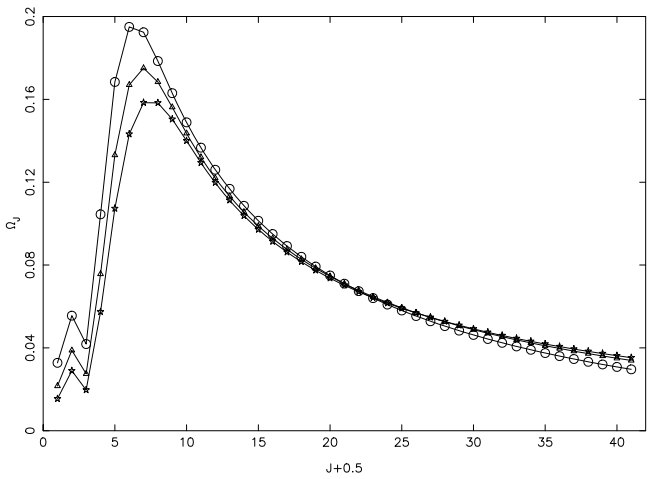

Fig. 1. Partial collision strengths for the 1s2s $^3S_1$–1s2p $^3P^\circ_1$ (2–4) transition of O VII, at three energies of: 60 Ryd (circles), 70 Ryd (triangles), and 80 Ryd (stars).

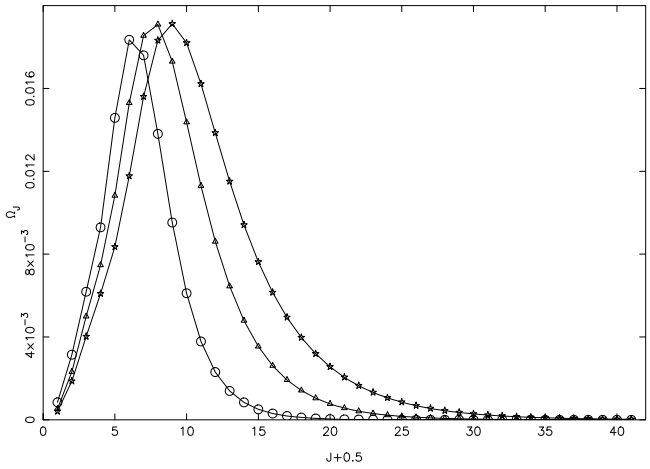

Fig. 2. Partial collision strengths for the 1s2s $^3S_1$–1s3p $^3P^\circ_1$ (2–10) transition of O VII, at three energies of: 60 Ryd (circles), 70 Ryd (triangles), and 80 Ryd (stars).

respectively, and at three energies of 60, 70, and 80 Ryd. Values of Ω have fully converged for all *resonance* transitions, including the allowed ones. Values of Ω have also converged for allowed transitions among the higher excited levels, as shown in Fig. 2 for the 2–10 transition. It is also clear from Fig. 2 that the need to include a larger range of partial waves increases with increasing energy. However, values of Ω have not converged for those allowed transitions whose ΔE is very small (mainly within the same n complex), as shown for the 2–4 transition in Fig. 1. Similarly, values of Ω have (almost) converged for all forbidden transitions, including those whose ΔE is very small, such as the 9–11 transition shown in Fig. 3. Therefore, only for the allowed transitions within the same n complex, our wide range of partial waves is not sufficient for the convergence of Ω, for which a top-up has been included as mentioned above.

In Table 5 we list our values of Ω for resonance transitions at energies *above* thresholds. The *indices* used to represent the levels of a transition have already been defined in Table 1. No comparisons can be made with our calculations because Delahaye & Pradhan (2002) have not reported results for collision strengths. Therefore, in order to make an accuracy assessment of the

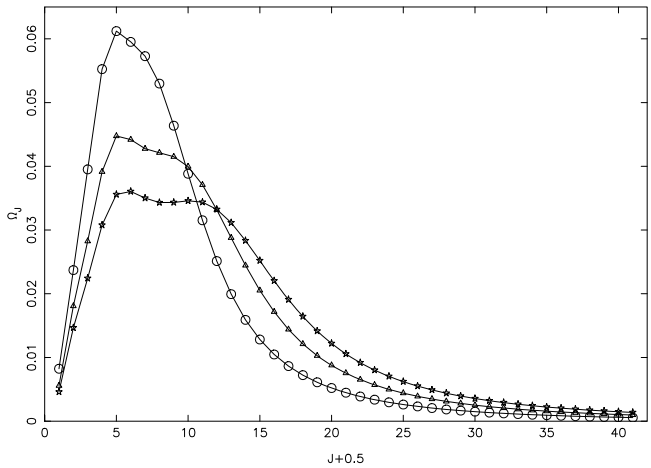

Fig. 3. Partial collision strengths for the 1s3p $^3P^\circ_0$–1s3p $^3P^\circ_2$ (9–11) transition of O VII, at three energies of: 60 Ryd (circles), 70 Ryd (triangles), and 80 Ryd (stars).

values of Ω, we have performed another calculation using the FAC code of Gu (2003). This code is also fully relativistic, and is based on the well known and widely used *distorted-wave* (DW) method. Furthermore, the same CI is included in FAC as in the calculations from DARC. Therefore, also included in Table 5 for a ready comparison are the Ω values from FAC at a single *excited* energy (E_j) of ∼75 Ryd, corresponding to the *incident* energy of ∼120 Ryd. Generally the two sets of Ω agree well, but differences for four transitions, namely 1–27, 1–29, 1–41, and 1–43, are over 30%, and the discrepancy is an order of magnitude for two transitions, namely 1–45 and 1–47. However, all these transitions are very *weak* ($\Omega \leq 10^{-6}$). The contribution of such weak transitions in any modelling application is likely to be insignificant.

In Fig. 4 we show the variation of our values of Ω with energy for three *allowed* transitions, namely 2–5 (1s2s $^3S_1$–1s2p $^3P^\circ_2$), 4–14 (1s2p $^3P^\circ_1$–1s3d $^3D_2$), and 10–24 (1s3p $^3P^\circ_1$–1s4d $^3D_2$). Also included in this figure are the corresponding results obtained from the FAC code. It may be noted that our calculations from DARC are only up to E = 140 Ryd (see Sect. 6) whereas the FAC calculates Ω up to ∼500 Ryd. For all the above three (and many other) transitions there are no discrepancies between the f-values obtained from the two independent (GRASP and FAC) codes, and therefore the Ω values also agree to better than 20%. However, the Ω values obtained from FAC are slightly anomalous, particularly towards the lower end of the energy range, and the agreement between the two calculations improves with increasing energy. Such occasional anomalies for a few random transitions occur because of the interpolation and extrapolation techniques employed in the FAC code, which is designed to generate a large amount of atomic data in a comparatively very short period of time, and without too much loss of accuracy. Similarly, some difference in the values of Ω are expected because the DW method generally overestimates the results for light ions due to the exclusion of channel coupling.

Similar comparisons between the two calculations are made in Fig. 5 for three *forbidden* transitions, namely 2–8 (1s2s $^3S_1$–1s3s $^3S_1$), 2–15 (1s2s $^3S_1$–1s3d $^3D_3$), and 4–10 (1s2p $^3P^\circ_1$–1s3p $^3P^\circ_1$). For these transitions, the agreement between the two calculations also improves with increasing energy. Therefore, in some instances a problem of a few anomalies may arise from the calculations from FAC, but overall we observe no discrepancy with our

Table 5. Collision strengths for resonance transitions of O VII. ($a \pm b \equiv a \times 10^{\pm b}$).

Transition		Energy (Ryd)						
i	j	60	70	80	100	120	140	FAC
1	2	2.786−3	2.322−3	1.942−3	1.461−3	1.129−3	9.092−4	1.089−3
1	3	1.534−3	1.193−3	9.460−4	6.141−4	4.273−4	3.109−4	3.973−4
1	4	4.598−3	3.576−3	2.837−3	1.845−3	1.287−3	9.400−4	1.201−3
1	5	7.628−3	5.927−3	4.699−3	3.048−3	2.120−3	1.542−3	1.980−3
1	6	9.337−3	1.016−2	1.077−2	1.180−2	1.252−2	1.305−2	1.178−2
1	7	3.701−2	4.592−2	5.412−2	6.785−2	7.978−2	9.023−2	8.016−2
1	8	9.065−4	7.043−4	5.721−4	4.155−4	3.167−4	2.523−4	2.709−4
1	9	4.878−4	3.748−4	2.948−4	1.894−4	1.306−4	9.421−5	1.063−4
1	10	1.462−3	1.123−3	8.837−4	5.681−4	3.925−4	2.839−4	3.203−4
1	11	2.427−3	1.864−3	1.466−3	9.406−4	6.484−4	4.674−4	5.298−4
1	12	1.821−3	2.023−3	2.180−3	2.467−3	2.682−3	2.845−3	2.493−3
1	13	1.638−4	1.098−4	7.754−5	4.267−5	2.659−5	1.791−5	2.385−5
1	14	2.744−4	1.859−4	1.334−4	7.735−5	5.201−5	3.866−5	4.706−5
1	15	3.804−4	2.548−4	1.798−4	9.892−5	6.161−5	4.149−5	5.555−5
1	16	5.044−4	5.912−4	6.933−4	8.814−4	1.033−3	1.153−3	9.166−4
1	17	6.458−3	8.257−3	9.894−3	1.255−2	1.484−2	1.684−2	1.597−2
1	18	4.280−4	3.094−4	2.452−4	1.734−4	1.294−4	1.026−4	1.054−4
1	19	2.115−4	1.613−4	1.264−4	8.045−5	5.517−5	3.970−5	4.254−5
1	20	6.338−4	4.836−4	3.788−4	2.414−4	1.657−4	1.195−4	1.283−4
1	21	1.053−3	8.029−4	6.284−4	3.998−4	2.740−4	1.970−4	2.119−4
1	22	7.265−4	7.901−4	8.585−4	9.626−4	1.046−3	1.114−3	9.677−4
1	23	9.500−5	6.304−5	4.438−5	2.424−5	1.504−5	1.012−5	1.299−5
1	24	1.586−4	1.057−4	7.498−5	4.202−5	2.718−5	1.934−5	2.354−5
1	25	2.206−4	1.463−4	1.029−4	5.617−5	3.486−5	2.343−5	3.027−5
1	26	5.495−6	3.063−6	1.960−6	9.505−7	5.344−7	3.339−7	4.619−7
1	27	1.055−5	7.241−6	6.065−6	5.220−6	5.006−6	5.009−6	3.308−6
1	28	9.845−6	5.485−6	3.510−6	1.701−6	9.558−7	5.970−7	8.304−7
1	29	1.289−5	9.663−6	8.786−6	8.407−6	8.496−6	8.732−6	5.305−6
1	30	2.652−4	2.809−4	3.188−4	4.009−4	4.756−4	5.419−4	4.422−4
1	31	2.423−3	3.130−3	3.749−3	4.787−3	5.666−3	6.421−3	6.029−3
1	32	2.427−4	1.643−4	1.265−4	8.751−5	6.467−5	5.118−5	5.025−5
1	33	1.122−4	8.365−5	6.473−5	4.097−5	2.793−5	2.005−5	2.073−5
1	34	3.362−4	2.507−4	1.941−4	1.229−4	8.392−5	6.035−5	6.253−5
1	35	5.586−4	4.163−4	3.220−4	2.036−4	1.387−4	9.951−5	1.032−4
1	36	4.065−4	4.309−4	4.595−4	5.167−4	5.554−4	5.908−4	4.970−4
1	37	5.569−5	3.623−5	2.536−5	1.381−5	8.550−6	5.745−6	7.286−6
1	38	9.290−5	6.063−5	4.269−5	2.370−5	1.515−5	1.065−5	1.292−5
1	39	1.293−4	8.409−5	5.883−5	3.201−5	1.981−5	1.331−5	1.697−5
1	40	4.671−6	2.547−6	1.615−6	7.794−7	4.374−7	2.731−7	3.762−7
1	41	9.145−6	5.904−6	4.703−6	3.801−6	3.500−6	3.377−6	2.311−6
1	42	8.370−6	4.562−6	2.891−6	1.395−6	7.826−7	4.885−7	6.763−7
1	43	1.221−5	8.651−6	7.571−6	6.983−6	6.891−6	6.894−6	4.364−6
1	44	1.595−7	5.615−8	2.942−8	1.143−8	5.888−9	3.599−9	4.133−9
1	45	3.659−7	1.829−7	1.308−7	1.416−7	2.443−7	3.509−7	2.197−8
1	46	2.497−7	8.783−8	4.600−8	1.786−8	9.206−9	5.626−9	6.489−9
1	47	4.071−7	2.113−7	1.546−7	1.740−7	3.047−7	4.392−7	2.526−8
1	48	1.553−4	1.528−4	1.689−4	2.100−4	2.490−4	2.842−4	2.356−4
1	49	1.299−3	1.643−3	1.956−3	2.477−3	2.926−3	3.306−3	3.024−3

results from the DARC code, as also found for many other ions, such as those of iron – see, for example, Aggarwal et al. (2008) and references therein. In conclusion, based on the discussion above and the comparisons made, we do not see any apparent deficiency in our calculations for Ω, and estimate our results to be accurate to better than 20% for a majority of the transitions.

6. Excitation rates

Excitation rates, along with energy levels and radiative rates, are required for plasma modelling, and are determined from the collision strengths (Ω). Since the threshold energy region is dominated by numerous closed-channel (Feshbach) resonances, values of Ω need to be calculated in a fine energy mesh in order to accurately account for their contribution. Furthermore, in a hot plasma electrons have a wide distribution of velocities, and therefore values of Ω are generally averaged over a *Maxwellian* distribution as follows:

$$\Upsilon(T_{\rm e}) = \int_0^\infty \Omega(E) \exp(-E_j/kT_{\rm e}) {\rm d}(E_j/kT_{\rm e}), \quad (7)$$

where k is Boltzmann constant, $T_{\rm e}$ is the electron temperature in K, and E_j is the electron energy with respect to the final (excited) state. Once the value of Υ is known the corresponding results for

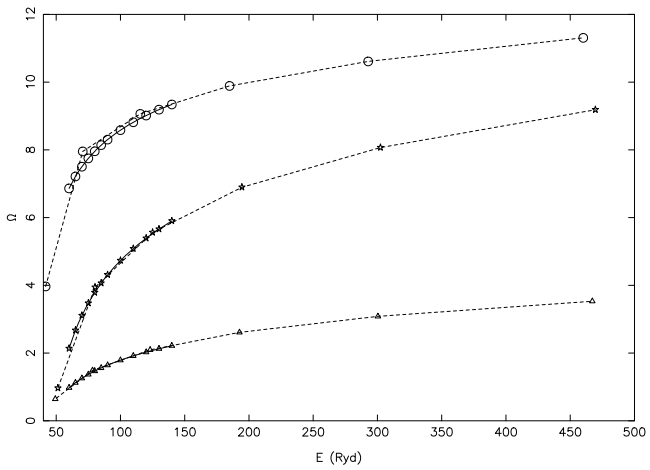

Fig. 4. Comparison of collision strengths from our calculations from DARC (continuous curves) and FAC (broken curves) for the 2–5 (circles: 1s2s ^{3}S$_1$–1s2p ^{3}P$^\circ_2$), 4–14 (triangles: 1s2p ^{3}P$^\circ_1$–1s3d ^{3}D$_2$), and 10–24 (stars: 1s3p ^{3}P$^\circ_1$–1s4d ^{3}D$_2$) allowed transitions of O VII .

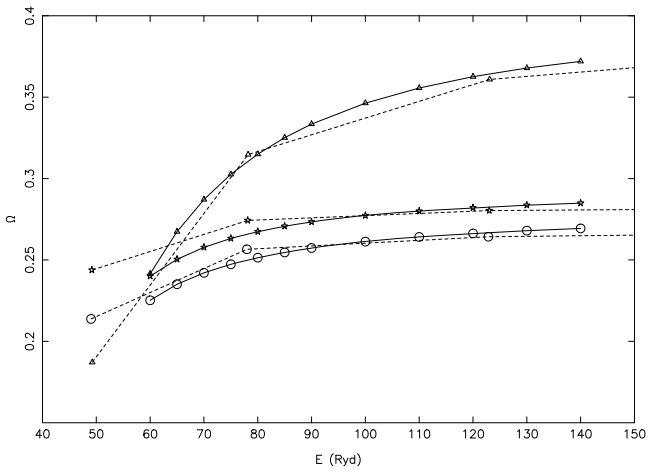

Fig. 5. Comparison of collision strengths from our calculations from DARC (continuous curves) and FAC (broken curves) for the 2–8 (circles: 1s2s ^{3}S$_1$–1s3s ^{3}S$_1$), 2–15 (triangles: 1s2s ^{3}S$_1$–1s3d ^{3}D$_3$), and 4–10 (stars: 1s2p ^{3}P$^\circ_1$–1s3p ^{3}P$^\circ_1$) forbidden transitions of O VII.

the excitation $q(i, j)$ and de-excitation $q(j, i)$ rates can be easily obtained from the following equations:

$$q(i,j) = \frac{8.63\times10^{-6}}{\omega_i T_{\rm e}^{1/2}} \Upsilon \exp(-E_{ij}/kT_{\rm e}) \qquad {\rm cm^3\ s^{-1}} \qquad (8)$$

and

$$q(j,i) = \frac{8.63\times10^{-6}}{\omega_j T_{\rm e}^{1/2}} \Upsilon \qquad {\rm cm^3\ s^{-1}}, \qquad (9)$$

where ω_i and ω_j are the statistical weights of the initial (i) and final (j) states, respectively, and E_{ij} is the transition energy. The contribution of resonances may enhance the values of Υ over those of the background values of collision strengths ($\Omega_{\rm B}$), especially for the forbidden transitions, by up to a factor of ten (or even more) depending on the transition and/or the temperature. Similarly, values of Ω need to be calculated over a wide energy range (above thresholds) in order to obtain convergence of the integral in Eq. (7), as demonstrated in Fig. 7 of Aggarwal & Keenan (2008).

The temperature of maximum abundance in ionisation equilibrium for O VII is $10^{5.9}$ K (Bryans et al. 2008), while our range of energy (up to 80 Ryd) is sufficient to calculate values of Υ up to $T_{\rm e} = 10^6$ K. However, we have extended our energy range up to 140 Ryd by performing another calculation from DARC, but with a smaller R-matrix radius of 12.0 au. Values of Ω obtained from this calculation differ insignificantly in the $60 \le E \le 80$ Ryd energy range from those already described. This exercise enables us to extend the temperature range of our calculations for Υ up to $T_{\rm e} = 2\times10^6$ K.

To delineate resonances, we have performed our calculations of Ω at over 4200 energies in the threshold region. Close to thresholds (~0.1 Ryd above a threshold) the energy mesh is 0.001 Ryd, and away from thresholds is 0.002 Ryd. Thus care has been taken to include as many resonances as possible, and with as fine a resolution as is computationally feasible. The density and importance of resonances can be appreciated from Figs. 6 a–f and 7 a–f, where we show our values of Ω in the thresholds region for some resonance transitions, namely 1–2, 4, 5, 7, 8, 10, 11, 13, 14, 15, 16, and 17. These transitions have been chosen because Delahaye & Pradhan (2002) have also shown similar resonances, and hence comparisons can be made between the two calculations. The density and magnitude of resonances between our calculations and those of Delahaye & Pradhan are comparable for some transitions, such as: 1–7, 10,11, and 17, i.e. Figs. 6d,f, and 7a,f, respectively. However, for some transitions, such as: 1–2, 4, 5, and 8, i.e. Figs. 6a–c, and e, respectively, resonances in our calculations are denser, particularly at energies just above the thresholds. This is mainly because *fine-structure* is explicitly included in the definition of channel coupling, which takes account of the relativistic effects in a more accurate way, and is particularly beneficial for splitting the terms of a state. However, the size of the Hamiltonian increases correspondingly, hence making the calculations computationally more expensive. These near threshold resonances affect the values of Υ particularly towards the lower end of the temperature range, which we discuss below.

Our calculated values of Υ are listed in Table 6 over a wide temperature range of $1.0\times10^4 \le T_{\rm e} \le 2.0\times10^6$ K, suitable for applications in solar and other plasmas. The most recent and sophisticated calculations available for comparison are by Delahaye & Pradhan (2002), as stated in Sect. 1. They employed the R- matrix code but in a Breit-Pauli approximation, which should be sufficient to account for the relativistic effects for light ions, such as O VII. They also resolved resonances in the thresholds region to account for their contribution in the determination of Υ values, and included a wide energy range for calculating values of Ω in order to ensure the convergence of the integral in Eq. (7) at all temperatures. Finally, they included contributions of all partial waves with $J \le 17.5$ to obtain converged values of collision strengths. This limited range of partial waves is *insufficient* for the convergence of Ω values, particularly for transitions among the excited levels, as discussed in Sect. 5 and demonstrated in Figs. 1–3. However, this range of partial waves is fully sufficient for the convergence of Ω for all *resonance* transitions. Hence the Υ values of Delahaye & Pradhan should be comparatively more reliable for the resonance transitions.

Delahaye & Pradhan (2002) have not reported results for Ω or Υ, but their results for Υ are available electronically on the TIPbase website (`http://vizier.u-strasbg.fr/tipbase/home.html`), as noted in Sect. 1. However, before we discuss comparisons between their and our results, we point out that the values of Υ shown in their Figs. 6–8 and those available on the TIPbase website are not compatible for some transitions, such as

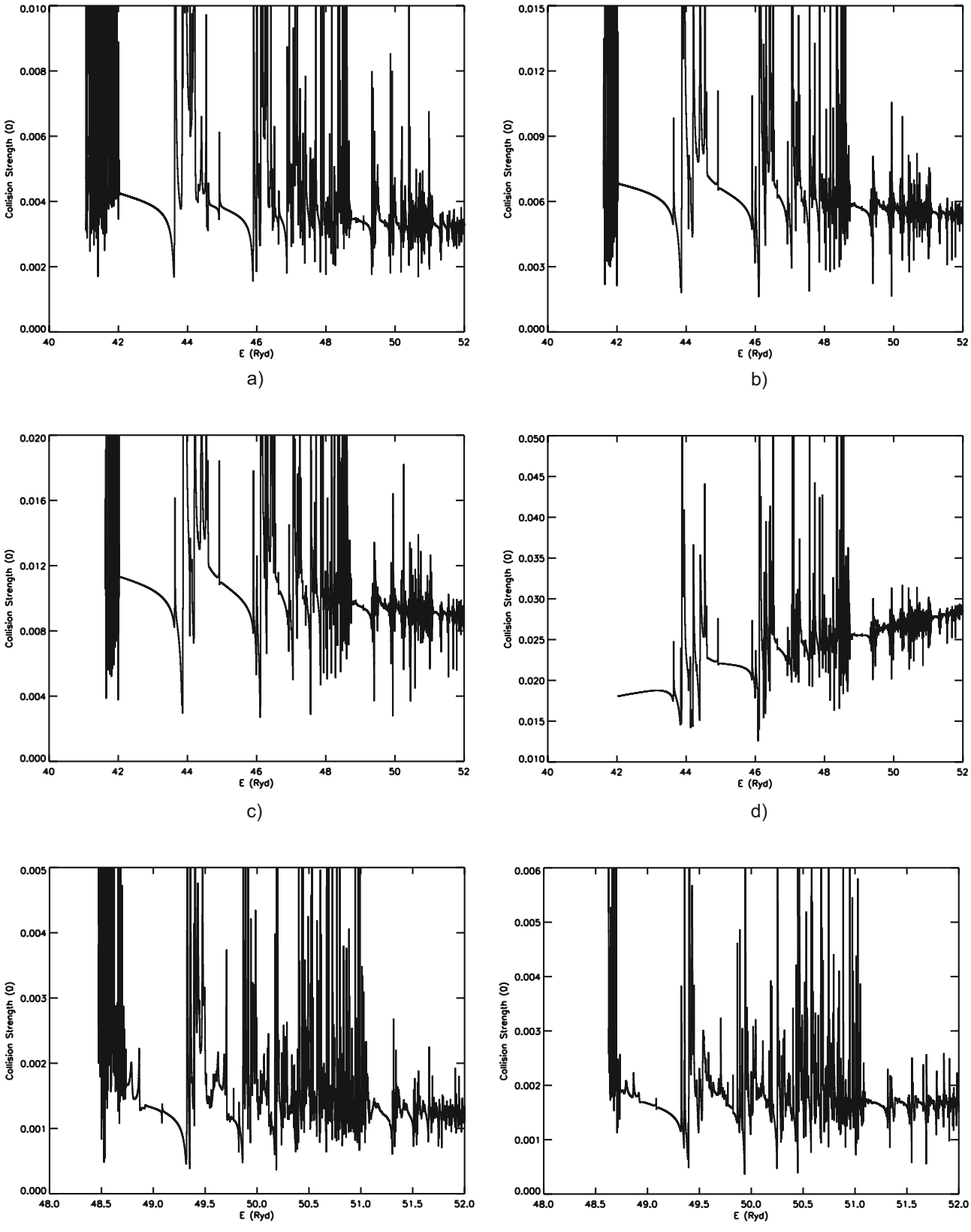

Fig. 6. **a)** Collision strengths for the $1s^2\ {}^1S_0$–$1s2s\ {}^3S_1$ (1–2) transition of O VII. **b)** Collision strengths for the $1s^2\ {}^1S_0$–$1s2p\ {}^3P^\circ_1$ (1–4) transition of O VII. **c)** Collision strengths for the $1s^2\ {}^1S_0$–$1s2p\ {}^3P^\circ_2$ (1–5) transition of O VII. **d)** Collision strengths for the $1s^2\ {}^1S_0$–$1s2p\ {}^1P^\circ_1$ (1–7) transition of O VII. **e)** Collision strengths for the $1s^2\ {}^1S_0$–$1s3s\ {}^3S_1$ (1–8) transition of O VII. **f)** Collision strengths for the $1s^2\ {}^1S_0$–$1s3p\ {}^3P^\circ_1$ (1–10) transition of O VII.

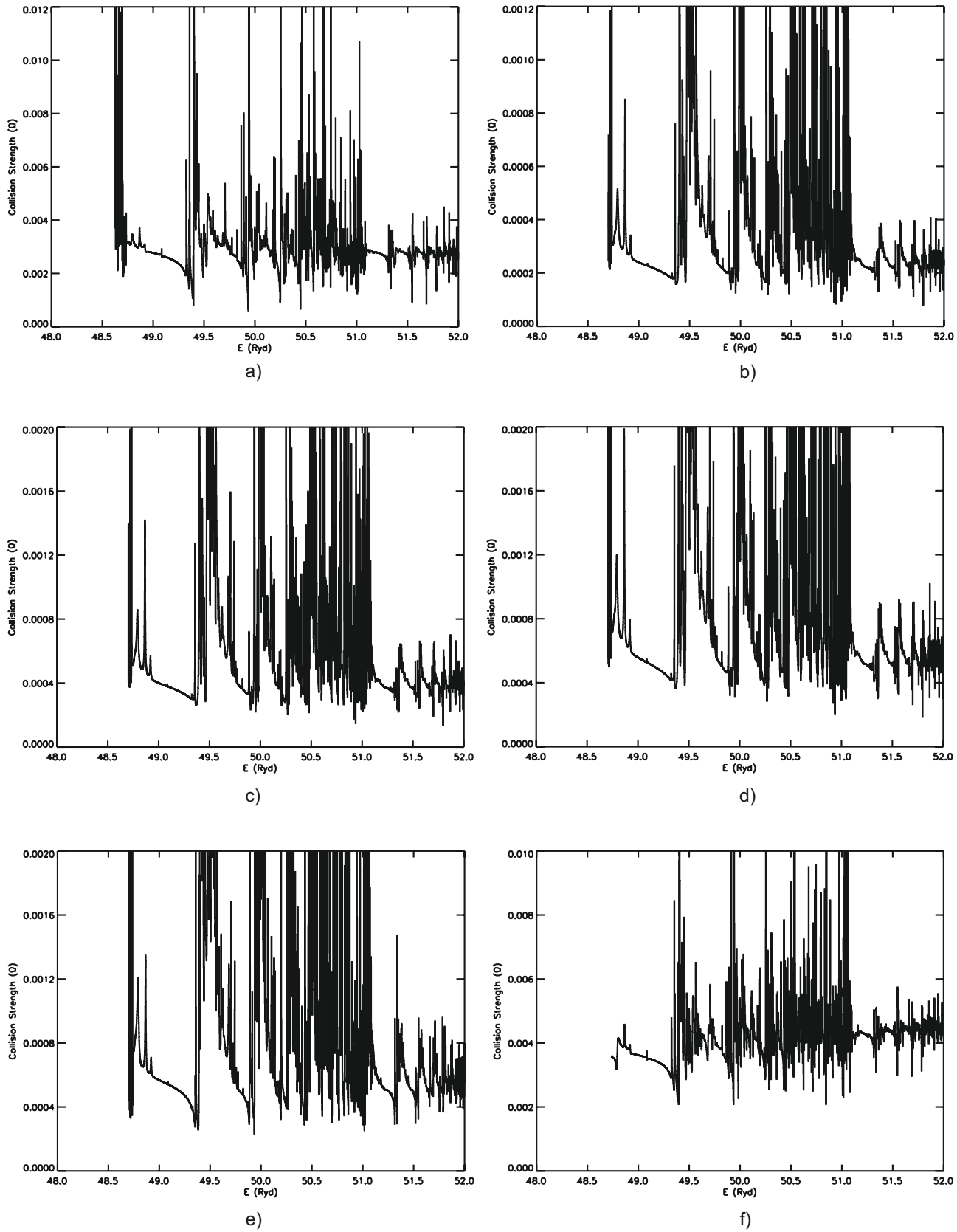

Fig. 7. **a)** Collision strengths for the $1s^2\ ^1S_0$–$1s3p\ ^3P^o_2$ (1–11) transition of O VII. **b)** Collision strengths for the $1s^2\ ^1S_0$–$1s3d\ ^3D_1$ (1–13) transition of O VII. **c)** Collision strengths for the $1s^2\ ^1S_0$–$1s3d\ ^3D_2$ (1–14) transition of O VII. **d)** Collision strengths for the $1s^2\ ^1S_0$–$1s3d\ ^3D_3$ (1–15) transition of O VII. **e)** Collision strengths for the $1s^2\ ^1S_0$–$1s3d\ ^1D_2$ (1–16) transition of O VII. **f)** Collision strengths for the $1s^2\ ^1S_0$–$1s3p\ ^1P^o_1$ (1–17) transition of O VII.

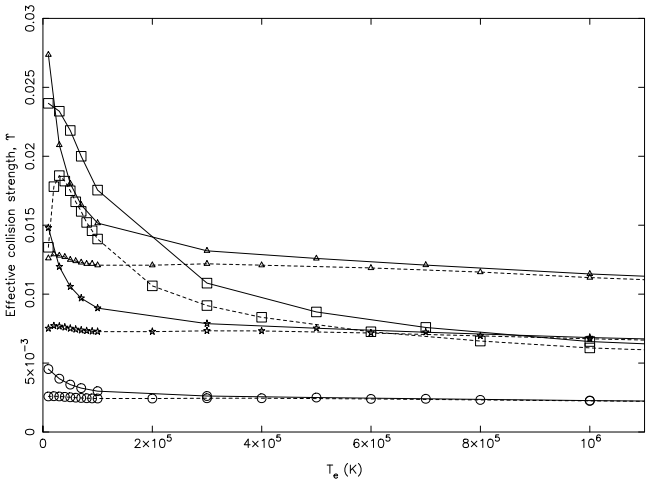

Fig. 8. Comparison of effective collision strengths from our calculations from DARC (continuous curves) and those of Delahaye & Pradhan (2002: broken curves) for the 1–2 (squares: $1s^2\ ^1S_0$–$1s2s\ ^3S_1$), 1–3 (circles: $1s^2\ ^1S_0$–$1s2p\ ^3P^o_0$), 1–4 (stars: $1s^2\ ^1S_0$–$1s2p\ ^3P^o_1$), and 1–5 (triangles: $1s^2\ ^1S_0$–$1s2p\ ^3P^o_2$) transitions of O VII.

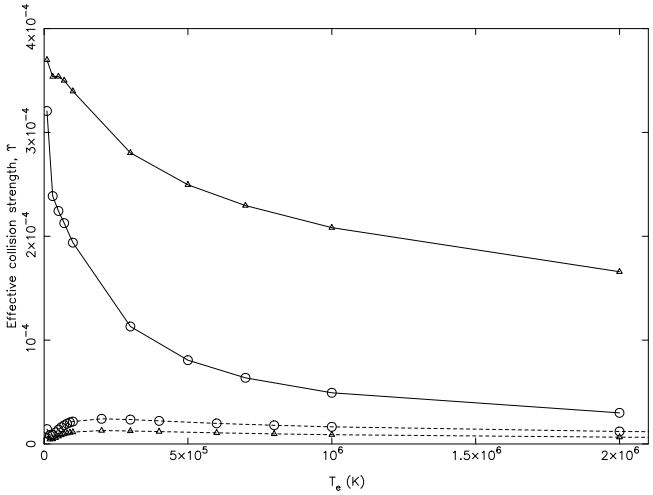

Fig. 9. Comparison of effective collision strengths from our calculations from DARC (continuous curves) and those of Delahaye & Pradhan (2002: broken curves) for the 1–24 (triangles: $1s^2\ ^1S_0$–$1s4d\ ^3D_2$) and 1–27 (circles: $1s^2\ ^1S_0$–$1s4f\ ^3F^o_3$) transitions of O VII.

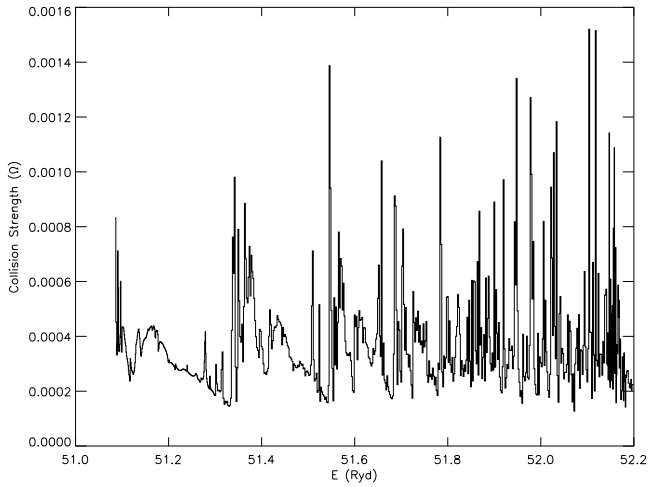

Fig. 10. Collision strengths for the $1s^2\ ^1S_0$–$1s4d\ ^3D_2$ (1–24) transition of O VII.

4–6 ($1s2p\ ^3P^o_1$–$1s2s\ ^1S_0$), 4–13 ($1s2p\ ^3P^o_1$–$1s3d\ ^3D_1$), and 8–14 ($1s3s\ ^3S_1$–$1s3d\ ^3D_2$). For the 4–13 transition we assume this corresponds to $1s2p\ ^3P^o_1$–$1s3d\ ^3D_1$, rather than $1s2p\ ^3P^o_1$–$2\ ^3D_1$ as labelled by Delahaye & Pradhan. Nevertheless, a comparison of their results with ours indicates that the Υ values listed on the website are correct, and therefore we will discuss comparisons with those results alone.

A comparison between our Υ values and those of Delahaye & Pradhan (2002) shows differences of over 20% for almost all (89% to be precise) the 465 *common* transitions among the lowest 31 levels, in the common temperature range of $1.0 \times 10^4 \leq T_e \leq 2.0{\times}10^6$ K. Since resonance transitions are the most important and probably the most accurate among those calculated by Delahaye & Pradhan, as discussed above, we focus on a comparison for these transitions. Temperatures towards the lower end are particularly sensitive to the presence (or absence) of those resonances which are near the thresholds, as shown in Fig. 6 (a–c and e–f). To demonstrate this, we compare the two sets of Υ for the 1–2, 3, 4, and 5 transitions in Fig. 8. For all these (and many other) transitions the discrepancy is the largest (up to a factor of two) at the lowest temperature, and decreases with increasing temperature. Our larger values of Υ for such transitions are understandable for the reasons discussed above, and are clearly due to the denser resonances we observe in our calculations. However, transitions involving levels 23 and higher show even larger discrepancies of up to an order of magnitude, and particularly notable are four, namely 1–24, 27, 29, and 31. Since the discrepancy is the largest for the 1–24 ($1s^2\ ^1S_0$–$1s4d\ ^3D_2$) and 1–27 ($1s^2\ ^1S_0$–$1s4f\ ^3F^o_3$) transitions, we focus our comparison on these to understand the differences.

In Fig. 9 we show our values of Υ and those of Delahaye & Pradhan (2002) for both the 1–24 and 1–27 transitions. Since our values of Υ are consistently higher over the entire temperature range, the first suspicion is that the differences are due to resonances, because we have included an additional 18 levels of the $n = 5$ configurations, whereas Delahaye & Pradhan have not. These transitions do show resonances over the entire threshold energy range, as shown for illustration in Fig. 10 for the 1–24 transition for which the discrepancy is the largest. However, these resonances are neither dense nor very large in magnitude, and therefore the effect on the determination of Υ values is *not* very significant, especially at temperatures above 10^5 K. Hence, the differences between the two sets of Υ values probably arise from the differences in the corresponding values of Ω. Unfortunately, Delahaye & Pradhan have not reported their results for Ω, except for a few transitions in graphical form. However, for a majority of the transitions, and particularly the resonance lines, there is no (large) discrepancy between our calculations from DARC and FAC, as discussed already in Sect. 5 and may also be noted from Table 5. Furthermore, our values of Ω and Υ decrease with increasing energy (temperature), as both of these are forbidden transitions. However, this is not so much apparent in the calculations of Delahaye & Pradhan. Therefore, we have confidence in our results. Finally, we note that even over the higher temperature range ($1.0 \times 10^5 \leq T_e \leq 2.0 \times 10^6$ K), differences between our values of Υ and those of Delahaye & Pradhan are over 20% for about 80% of the transitions in common. Differences of about an order of magnitude are common for many transitions, but are particularly large (up to two orders of magnitude) for six, namely 2–24, 25; 21–24, 23–26, 24–27, and 27–30. Most of the differences are (perhaps) due to

the differences in the corresponding values of Ω, because the limited range of partial waves ($J \leq 17.5$) adopted by Delahaye & Pradhan is inadequate for the convergence of Ω for a large number of forbidden and most of the allowed transitions among excited levels, as discussed earlier in Sect. 5.

7. Conclusions

In this paper we have presented results for energy levels and radiative rates for four types of transitions (E1, E2, M1, and M2) among the lowest 49 levels of O VII belonging to the $n \leq 5$ configurations. Additionally, lifetimes of all the levels have been reported, although measurements are available for only a few, for which there is no discrepancy between theory and experiments. Based on a variety of comparisons, our energy levels are assessed to be accurate to better than 0.5%, and the results for radiative rates, oscillator strengths, line strengths, and lifetimes are assessed to be accurate to better than 20% for a majority of the strong transitions (levels). Similarly, the accuracy of our results for collision strengths and effective collision strengths is estimated to be better than 20% for a majority of the transitions. This accuracy estimate is based on a comparison between two independent calculations performed with the DARC and FAC codes. Additionally, we have considered a large range of partial waves in order to achieve the convergence of values of Ω at all energies, included a wide energy range in order to accurately calculate the values of Υ up to $T_e = 2.0 \times 10^6$ K, and resolved resonances in a fine energy mesh in order to account for their contributions. Hence, overall improvements have been made over the earlier available Υ results of Delahaye & Pradhan (2002), which differ from the present calculations by over an order of magnitude for many transitions. Finally, we have also included the additional 18 levels of the $n = 5$ configurations, which have helped to improve the accuracy of the values of Υ for all those transitions whose levels belong to the $n \leq 4$ configurations. Similarly, our present results for transitions involving the levels of the $n = 5$ configurations can be further improved by the inclusion of the levels of the $n = 6$ configurations. We believe the present set of complete results for radiative and excitation rates are the most reliable currently available, and will be highly useful for the modelling of a variety of plasmas.

Acknowledgements. This work has been financed by the Engineering and Physical Sciences and Science and Technology Facilities Councils of the United Kingdom, and F.P.K. is grateful to A. W. E. Aldermaston for the award of a William Penney Fellowship. We thank Dr. P. H. Norrington for providing his revised GRASP and DARC codes prior to publication.

References

Acton, L. W., Catura, R. C., Meyerott, A. J., Wolfson, C. J., & Culhane, J. L. 1972, Sol. Phys., 26, 183
Aggarwal, K. M., & Keenan, F. P. 2008, Eur. Phys. J., D 46, 205
Aggarwal, K. M., Tayal, V., Gupta, G. P., & Keenan, F. P. 2007, ADNDT, 93, 615
Aggarwal, K. M., Hamada, K., Igarashi, A., et al. 2008, A&A, 484, 879
Baker, S. C. 1973, J. Phys. B, 6, 709
Berrington, K. A., Eissner, W. B., & Norrington, P. H. 1995, Comput. Phys. Commun., 92, 290
Bryans, P., Landi, E., & Savin, D. W. 2008, ApJ, in press [arXiv:0805.3302]
Delahaye, F., & Pradhan, A. K. 2002, J. Phys. B, 35, 3377
Dere, K. P., Landi, E., Young, P. R., & Del Zanna G. 2001, ApJS, 134, 331
Eissner, W., Jones, M., & Nussbaumer, H. 1974, Comput. Phys. Commun., 8, 270
Gabriel, A. H., & Jordan, C. 1969, MNRAS, 145, 241
Grant, I. P., McKenzie, B. J., Norrington, P. H., Mayers, D. F., & Pyper, N. C. 1980, Comput. Phys. Commun., 21, 207
Gu, M. F. 2003, ApJ, 582, 1241
Hibbert, A. 1996, Phys. Scr., T65, 104
Hibbert, A. 2000, AIP Conf. Proc., 543, 242
Isler, R. C., Jupen, C., & Martinson, I. 1993, Phys. Scr., 47, 32
Keenan, F. P., Kingston, A. E., & McKenzie, D. L. 1985, ApJ, 291, 855
McKenzie, D. L., Landecker, P. B., Broussard, R. M., et al. 1980, ApJ, 241, 409
Phillips, K. J. H., Mewe, R., Harra-Murnion, L. K., et al. 1999, A&AS, 138, 381
Savukov, I. M., Johnson, W. R., & Safranova, U. I. 2003, ADNDT, 85, 83
Träbert, E., Heckmann, P. H., & Buttlar, H. V. 1977, Z. Phys. A, 280, 11
Winkler, P. F., Clark, G. W., Markert, T. H., Petre, R., & Canizares, C. R. 1981, ApJ, 245, 574